Am J Physiol Cell Physiol 304: C342–C353, 2013.
First published December 12, 2012; doi:10.1152/ajpcell.00153.2012.

Endoplasmic reticulum stress signal impairs erythropoietin production: a role for ATF4

Chih-Kang Chiang,[1,2] Masaomi Nangaku,[1] Tetsuhiro Tanaka,[1] Takao Iwawaki,[3] and Reiko Inagi[1]

[1]*Division of Nephrology and Endocrinology, The University of Tokyo School of Medicine, Tokyo, Japan;* [2]*Division of Nephrology, Department of Internal Medicine, College of Medicine, National Taiwan University, Taipei, Taiwan; and* [3]*Iwawaki Laboratory, Advanced Scientific Research Leaders Development Unit, Gunma University, Gunma, Japan*

Submitted 27 April 2012; accepted in final form 28 November 2012

Chiang CK, Nangaku M, Tanaka T, Iwawaki T, Inagi R. Endoplasmic reticulum stress signal impairs erythropoietin production: a role for ATF4. *Am J Physiol Cell Physiol* 304: C342–C353, 2013. First published December 12, 2012; doi:10.1152/ajpcell.00153.2012.—Hypoxia upregulates the hypoxia-inducible factor (HIF) pathway and the endoplasmic reticulum (ER) stress signal, unfolded protein response (UPR). The cross talk of both signals affects the pathogenic alteration by hypoxia. Here we showed that ER stress induced by tunicamycin or thapsigargin suppressed inducible ($CoCl_2$ or hypoxia) transcription of erythropoietin (EPO), a representative HIF target gene, in HepG2. This suppression was inversely correlated with UPR activation, as estimated by expression of the UPR regulator glucose-regulated protein 78, and restored by an ER stress inhibitor, salubrinal, in association with normalization of the UPR state. Importantly, the decreased EPO expression was also observed in HepG2 overexpressing UPR activating transcription factor (ATF)4. Overexpression of mutated ATF4 that lacks the transcriptional activity did not alter EPO transcriptional regulation. Transcriptional activity of the EPO 3′-enhancer, which is mainly regulated by HIF, was abolished by both ER stressors and ATF4 overexpression, while nuclear HIF accumulation or expression of other HIF target genes was not suppressed by ER stress. Chromatin immunoprecipitation analysis identified a novel ATF4 binding site (TGACCTCT) within the EPO 3′-enhancer region, suggesting a distinct role for ATF4 in UPR-dependent suppression of the enhancer. Induction of ER stress in rat liver and kidney by tunicamycin decreased the hepatic and renal mRNA and plasma level of EPO. Collectively, ER stress selectively impairs the transcriptional activity of EPO but not of other HIF target genes. This effect is mediated by suppression of EPO 3′-enhancer activity via ATF4 without any direct effect on HIF, indicating that UPR contributes to oxygen-sensing regulation of EPO.

unfolded protein response; hypoxia-inducible factor; activating transcription factor 4

HYPOXIA AND ITS STRESS RESPONSE, the hypoxia-inducible factor (HIF) pathway, play a crucial role in physiological and pathophysiological phenomena in various organs, including kidney, liver, heart, and brain, and thereby link to ischemic diseases (6, 27, 28, 32, 35). Erythropoietin (EPO), produced by the kidney and liver, stimulates erythropoiesis and increases oxygen delivery to tissues, which are exposed to hypoxia. Expression of EPO is carefully regulated by oxygen tensions, which is sensed by the HIF pathway (24). However, some transcription factors, including NF-κB, are also known to alter EPO transcriptional regulation and thereby trigger derangement of HIF-dependent EPO production under certain pathogenic conditions (23).

Address for reprint requests and other correspondence: R. Inagi, Division of Nephrology and Endocrinology, Univ. of Tokyo School of Medicine, 7-3-1 Hongo, Bunkyo-ku, Tokyo 113-8655, Japan (e-mail: inagi-npr@umin.ac.jp).

Hypoxia further induces other stress signals derived from the endoplasmic reticulum (ER). The role of the ER in maintaining protein homeostasis includes regulation of the synthesis, folding, and trafficking of client proteins. ER dysfunction triggered by hypoxia or energy consumption causes an imbalance in protein-folding capacity and protein-folding load (referred to as ER stress), which triggers the accumulation of unfolded proteins in the ER and a subsequent stress signal, the unfolded protein response (UPR; Ref. 16). Although the UPR initially serves as an adaptive response that acts to enhance protein-folding capacity, degrades malfolded proteins, and attenuates translation, this physiological response recharacterizes to a pathogenic response when the ER stress crosses a certain strength and duration threshold. The primary function of the UPR at this pathogenic level is to induce an apoptotic response (36). Recent evidence, including our studies, has also demonstrated that the UPR acts in various cells to maintain ER homeostasis at the basal level and that an imbalanced pathogenic UPR state as a consequence of ER stress contributes to the progression of various hypoxic diseases (3, 7–9, 15, 20, 29, 34). Further, cross talk between the HIF and UPR pathways has been highlighted to be important for stress signal regulation (41). To date, however, no evidence has been found for a pathophysiological role of ER stress in the EPO-producing system, particularly with regard to a link between the UPR and EPO-producing capacity.

Here we hypothesized that ER stress contributes to oxygen-sensing machinery for EPO production. To test this, we evaluated changes in EPO transcriptional activity under ER stress conditions, namely UPR activation, in in vitro studies in the EPO-producing cell line HepG2 and in in vivo studies in rats administered with ER stress inducers. The current study for the first time demonstrated that UPR under ER stress conditions suppresses basal and hypoxia-induced transcription of EPO but not other HIF target genes. This suppression of EPO transcription is mediated by derangement of EPO 3′-enhancer activity via activating transcription factor (ATF)4, a transcriptional factor for UPR pathway, indicating that UPR contributes to oxygen-sensing regulation of EPO.

METHODS

Cell culture. The human hepatoma cell line HepG2 was obtained from RIKEN BioResource Center (Tsukuba, Japan) and maintained in DMEM (Nissui Seiyaku, Tokyo, Japan) at pH 7.4 containing 10% FBS (SAFH Biosciences, Lenexa, KS). The cells were cultured in humidified 95% air-5% CO_2 at 37°C with various stimuli, namely the chemical hypoxia inducer cobalt chloride ($CoCl_2$; 100 μM), the ER stress inducers tunicamycin (TUN; 4 μg/ml) or thapsigargin (THG; 50 ng/ml; Sigma-Aldrich, St. Louis, MO), and the ER stress inhibitor salubrinal (20 μM; Santa Cruz Biotechnology, Santa Cruz, CA). In

some experiments, the cells were also cultured in a hypoxic chamber (1% O_2; Astec, Tokyo, Japan). The cells were exposed to these stimuli for 12 h for evaluation of mRNA expression and nuclear fraction.

Lactate dehydrogenase-release assay. After cells were cultured in a 24-well plate (1×10^5) for 24 h, culture media were collected and the cells were lysed with 0.5% Triton X-100. Lactate dehydrogenase (LDH) concentration of the medium and cell lysates was measured using LDH Kainos (Kainos Laboratories, Tokyo, Japan) according to the manufacturer's protocol. The ratio of medium LDH to the sum of medium and cellular LDHs was used as a marker of cellular injury. Each group consisted of three assays, and the experiments were independently repeated four times.

RNA isolation and quantitative real-time PCR. Total RNA was isolated by RNAiso plus (Takara, Tokyo, Japan) according to the manufacturer's protocol and reverse-transcribed, and the amount of mRNAs was evaluated by quantitative real-time PCR. cDNA was synthesized using the ImProm-II reverse transcription system (Promega, Madison, WI) from 1 μg of template RNA in a 20-μl reaction volume. One microliter of cDNA was added to Thunderbird qPCR Mix (Toyobo) and subjected to PCR amplification (cycled 40 times at 95°C for 30 s, 60°C for 30 s, and 72°C for 30 s) in the iCycler system (Bio-Rad). The β-actin was employed as an internal control. PCR was conducted in triplicate for each sample. The sequences of primers used for human and rat EPO, glucose-regulated protein 78 (GRP78), C/enhancer-binding protein homologous protein (CHOP), β-actin mRNA, human vascular endothelial growth factor (VEGF), and human glucose transporter 1 (GLUT1) are shown in Table 1. Each group consisted of three assays, and the experiments were independently repeated four times.

Measurement of EPO protein. The culture supernatant of HepG2 cells was concentrated 10-fold by AmiconUltra-15 (EMD Millipore, Billerica, MA), and the concentration of EPO protein of the supernatant was measured by radioimmunoassay (Recombigen EPO kit; Mitsubishi Chemical Medience, Tokyo, Japan). The plasma EPO level of the experimental rats ($n = 5$ for each group) was determined by ELISA using a Quantikine Mouse/Rat Epo Immunoassay kit (MEP00; R&D Systems, Minneapolis, MN).

Luciferase assays. We previously constructed a hypoxia-responsive reporter vector (pHRE-luc) by subcloning tandem copies of the HRE from the rat VEGF gene into the 5′ region of the human minimum CMV-promoter-luciferase gene of pGL3-basic vector (Promega) (37). The human genomic EPO DNA (906 bp, GeneBank No. 007933.15: nt 38353551–38354456; see the schematic representation of EPO gene in Fig. 4*A*), which included the core sequence of the EPO 3′-enhancer region, was subcloned into the 3′-region of the luciferase gene of the pGL3-promoter vector (pEPO3′-luc). Five hundred nanograms of pHRE-luc or pEPO3′-luc were cotransfected with 25 ng of pTK-Renilla luciferase (Promega) into HepG2 cells (1×10^5) utilizing Lipofectamine LTX with Plus reagent (Invitrogen). In some experiments, 200 ng of ATF4 expression plasmid (pCAX-F-mATF4 or ATF4-mut, see *Functional analysis of ATF4*) and 300 ng of pHRE-luc, pEPO3′-luc, or CHOP-luc (see *Functional analysis of ATF4*) were also cotransfected. The transfected cells were exposed to the indicated stimuli for 16 h and then lysed in 150 μl of passive protein lysis buffer for dual-luciferase assay. Measurement was done using a Lumat 9507 luminometer (EG and Berthold, Bad Wildbad, Germany). Transfection efficiency was corrected by dividing the relative value of the firefly luciferase light unit by that of the Renilla luciferase. Each group consisted of three assays, and the experiments were independently repeated four times.

Nuclear extract preparation. Nuclear or cytoplasmic proteins were extracted from HepG2 cells using the Thermo Scientific NE-PER nuclear and cytoplasmic extraction kit protocol after the addition of a protease inhibitor cocktail (Themo Fisher Scientific, Rockford, IL). Each extract was stored at −80°C until use. Protein concentrations were determined using the Bradford method with BSA as standard.

Western blot analyses. For detection of HIF-1α, HIF-2α, or ATF4, 30 μg of nuclear extract protein were loaded in each lane. These protein samples were separated by electrophoresis on an 8% (for HIF) or 10% (for ATF4) SDS-polyacrylamide gel and then electrotransfered to PVDF membranes (GE Healthcare Bio-Sciences, Little Chalfont, UK). The transferred membranes were blocked with 5% fat-free skim milk in TBS with 0.01% Tween 20 for 60 min at room temperature. The membranes were then incubated with rabbit polyclonal anti-HIF-1α, anti-HIF-2α (diluted 1:1,000; Novus Biologicals, Littleton, CO), or anti-ATF4 antibody, which raised against a peptide mapping near the COOH terminus of ATF4 (diluted 1:200; Santa Cruz Biotechnology) overnight at 4°C. Horseradish peroxidase-conjugated anti-rabbit IgG (Promega) was then used as the secondary antibody. Immunoreactive protein was visualized by the chemiluminescence protocol (ECL; GE Healthcare Bio-Sciences). Mouse monoclonal anti-histone H1 antibody (1:1,000; Santa Cruz) was used for calibration. Band intensity was assessed by densitometry using the ImageJ software (National Institutes of Health, Bethesda, MD). Each group consisted of four assays.

For detection of phosphorylation of eukaryotic initiation factor-2α (eIF2α), 30 μg of cytoplasmic proteins were separated by electrophoresis on 10% SDS-polyacrylamide gel, electrotransfered to PVDF membranes. The transferred membranes were blocked with 2% BSA, incubated with rabbit monoclonal anti-phospho-eIF2α (Ser51, 1:500) antibody or rabbit polyclonal anti-eIF2α antibody (1:500; Cell Signaling Technology, Danvers, MA) as a first antibody.

Functional analysis of ATF4. To evaluate the effect of ATF4 on EPO production, pCAX-F-mATF4 was established as an ATF4 expression plasmid by insertion of an F-mATF4 DNA fragment into the HindIII/XhoI sites of pCAX2. The F-mATF4 DNA fragment codes mouse full-length ATF4 (from 595 nt to 1,644 nt of NM_009716) with an NH_2-terminal FLAG tag and was produced by PCR using the primers (5′-CCC AAG CTT CCA CCA TGG ACT ACA AGG ACG ACG ATG ACA AGA CCG AGA TGA GCT TCC TGA ACA GC-3′ and 5′-CCG CTC GAG TTA CGG AAC TCT CTT CTT CCC CCT TGC CTT ACG-3′) and mouse ATF4 cDNA as a template. The

Table 1 *Primers used for quantitative real-time PCR*

Primer	Forward: 5′ to 3′	Reverse: 5′ to 3′
Human EPO	AGGCCGAGAATATCACGACG	CCATCCTCTTCCAGGCATAGAAA
Human VEGF	CCCTGATGAGATCGAGTACATCTT	TCTGAGCAAGGCCCACAGGGA
Human GLUT1	CTTCACTGTCGTGTCGCTGT	CCAGGACCCACTTCAAAGAA
Human GRP78	GCCTGTATTTCTAGACCTGCC	TTCATCTTGCCAGCCAGTTG
Human CHOP	ATGGCAGCTGAGTCATTGCCTTTC	AGAAGCAGGGTCAAGAGTGGTGAA
Human β-actin	TCCCCCAACTTGAGATGTATGAAG	AACTGGTCTCAAGTCAGTGTACAGG
Rat EPO	TACGTAGCCTCACTTCACTGCTT	GCAGAAAGTATCCGCTGTGAGTGTTC
Rat GRP78	CCCCAGATTGAAGTCACCTTTGAG	CAGGCGGTTTTGCTCATTG
Rat CHOP	CCAGCAGAGGTCACAAGCAC	CGCACTGACCACTCTGTTTC
Rat β-actin	CTTTCTACAATGAGCTGCGTG	TCATGAGGTAGTCTGTCAGG

EPO, erythropoietin; GLUT1, human glucose transporter 1; GRP, glucose-regulated protein 78; CHOP, C/enhancer-binding protein homologous protein.

expression plasmid of NH_2-terminal-deleted ATF4 (Δ2–144 aa), which lacks the transcriptional activity, was also used as an ATF4-mut (ca. 32 kDa). Neither of the ATF4 expression plasmids contains the upstream open reading frames. Plasmid transfection (500 ng) into HepG2 (1×10^5) was conducted using Lipofectamine LTX with Plus reagent (Invitrogen) and the resulting ATF4- or ATF4-mut-overexpressing HepG2 were assessed by real-time PCR, luciferase assay, or chromatin immunoprecipitation (ChIP) assay as described below. pCAX2 was employed as an empty control vector.

Transcriptional activity of ATF4 in HepG2-overexpressed ATF4 or ATF4-mut was estimated by luciferase assay utilizing CHOP-luc, which was constructed by introducing the two-tandem repeat of the

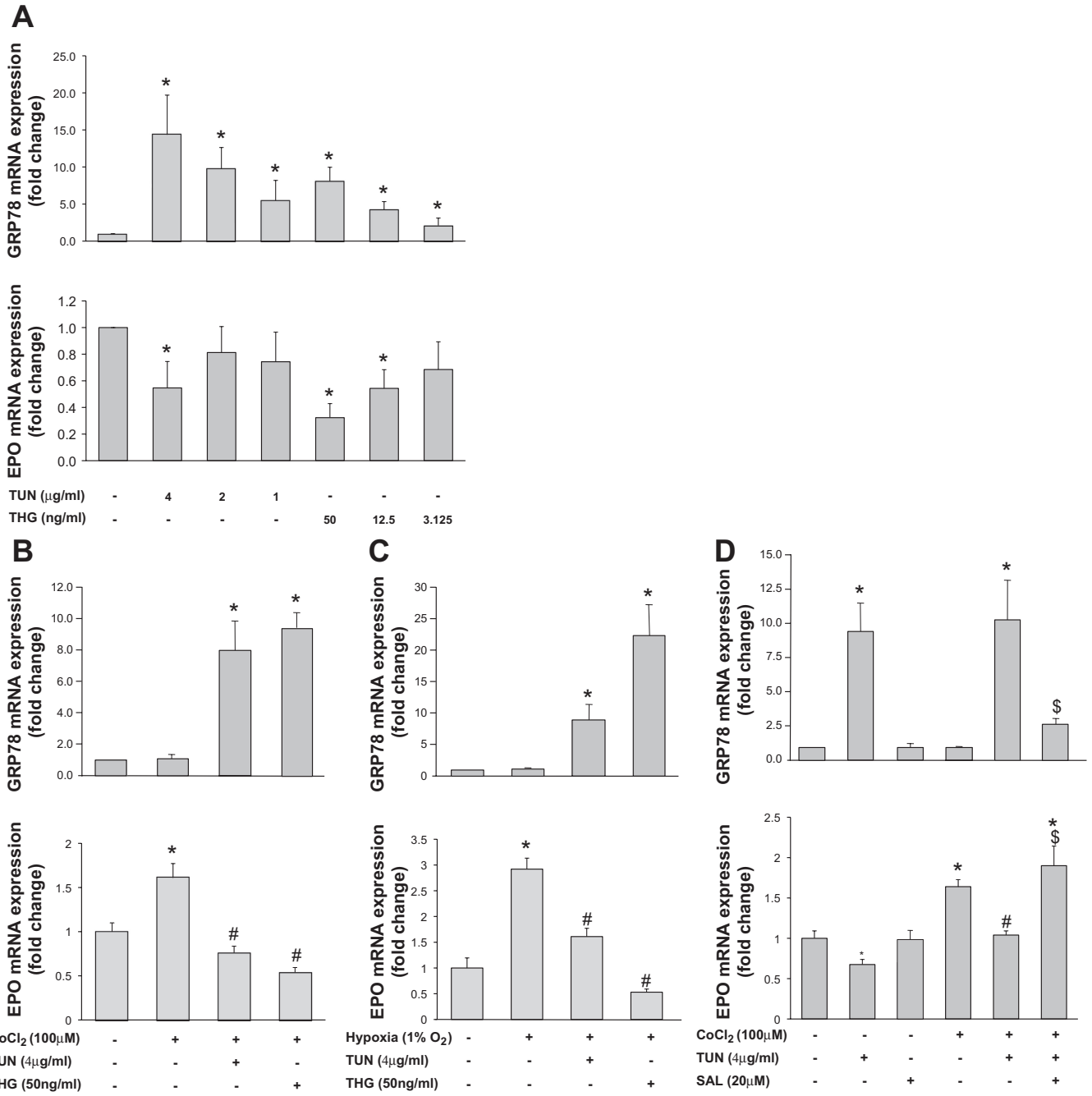

Fig. 1. Endoplasmic reticulum (ER) stress suppressed basal and inducible erythropoietin (EPO) transcription in HepG2 cells. *A*: when HepG2 cells were treated with a noncytotoxic dose of the ER stress inducers tunicamycin (TUN) or thapsigargin (THG) for 12 h under normoxia, the basal EPO mRNA level, which was measured by real-time PCR, was significantly suppressed in association with an increase in ER stress, as estimated by glucose-regulated protein 78 (GRP78) expression. *B* and *C*: under the condition of hypoxia-inducible factor (HIF) stabilization by 100 μM $CoCl_2$ (*B*) or hypoxia at 1.0% O_2 (*C*) for 12 h, EPO mRNA expression was significantly increased, while it was markedly blunted by TUN or THG. This suppression was inversely correlated with ER stress induction, as estimated by mRNA expression of GRP78. *D*: ER stress inhibitor salubrinal (SAL, 20μM) reduced the ER stress activation induced by TUN and normalized the UPR state (*top*), which was estimated by GRP78 mRNA level. In parallel, SAL restored basal and $CoCl_2$-induced EPO transcriptions, both of which were suppressed by TUN (*bottom*). Each group consisted of 3 assays, and the experiments were independently repeated 4 times. *$P < 0.05$, compared with untreated cells; #$P < 0.05$, compared with cells exposed to $CoCl_2$ or hypoxia alone; $$P < 0.05$, compared with cells treated with both $CoCl_2$ and TUN.

CHOP AARE element (aacATTGCATCAtccccgc) and TK promoter (−108 to +44) into pGL3-basic (Promega) with XhoI/ HindIII sites.

Small interfering RNA transfection. HepG2 cells were transfected with protein kinase RNA-like endoplasmic reticulum kinase (PERK) small interfering (si)RNA or control siRNA (EIF2AK3, Stealth RNAi; Invitrogen, Carlsbad, CA) utilizing HiPerFect transfection reagent (Qiagen, Tokyo, Japan). The level of PERK knockdown was evaluated by real-time PCR as described below. The PCR primers for PERK are Fw: 5′-CCT CAC CAT TTG CCT AAG GA-3′ and Rv: 5′-GGG GGA CTT TCC TTC TTC TG-3′.

Prediction of transcription factor binding site. The transcription factor binding site search in the EPO 3′-enhancer region was performed using the Transfac database (BIOBASE GmbH, Germany).

ChIP assay. HepG2 cells overexpressing FLAG-tagged ATF4 (pCAX-F-mATF4 transfectant) or mock (pCAX)-transfectant were subjected to hypoxia (1% O_2) for 8 h. ChIP was then performed with cross-linked chromatin from 4×10^6 cells and anti-FLAG antibody (M2, ×200; Sigma) using a SimpleChIP Enzymatic Chromatin IP kit (Cell Signaling Technology). Anti-histone H3 antibody (D2B12, ×100; Cell Signaling Technology) and anti-HIF-1α antibody (NB100–134, ×200; Novus Biologicals) were used as positive controls, and normal mouse IgG (×200; Sigma) was utilized as a negative control. The enriched chromatin DNA was quantified by PCR or real-time PCR with a TaqMan MGB probe (5′-FAM-TAC GCT GGT CAA TAA G-MGB-3′; Life Technologies, Tokyo, Japan). The primers used in this study were as follows: for PCR, forward primer (Pr 1), 5′-ACA CAG CCT GTC TGA CCT CTC GAC-3′, and reverse primer (Pr 2), 5′-TTG ATG ACA ATC TCA GCG CAC TGC-3′; for real-time PCR, forward primer (Pr 3), 5′-ACA GCC TGT CTG ACC TCT CGA C-3′, and reverse primer (Pr 4), 5′-CGG TGA GGC CTT GAA TGG-3′ (see Fig. 4*A*). The primers for human RPL30 Exon 3 (no. 7014; Cell Signaling Technology) and HRE of EPO 3′-enhancer region (forward primer, 5′- TAC GTG CTG TCT CAC ACA GCC TGT C-3′, and reverse primer, 5′-ACC TTA TTG ACC AGC GTA GGC AGA G-3′) were used as positive control primers. The amount of immunoprecipitated DNA in each sample was represented as a signal relative to the total amount of input chromatin, which was equivalent to one. We performed three independent experiments.

Animal experiments. Male Wistar rats weighing 200 g (Nippon Bio-Supp. Center, Tokyo, Japan) were subcutaneously injected with 60 mg/kg of $CoCl_2$ (Sigma) or vehicle (distilled water) and intraperitoneally with a nontoxic dose of TUN (0.3 mg/kg; Sigma; Ref. 15) or PBS and then killed 24 h later ($n = 5$ for each group). The renal cortex and liver parenchyma were harvested and stored at −80°C until use. All animal experiments were performed in accordance with the *National Institutes of Health Guidelines for the Use and Care of Laboratory Animals* and approved by the University of Tokyo Local Ethical Committee.

Immunohistochemistry. The ER stress state of tubulointerstitial cells in in vivo studies was evaluated by immunohistochemistry for the detection of GRP78 using renal cortical tissue sections (3-μm) fixed with methyl Carnoy's solution as previously described (15). Briefly, sections were incubated with goat polyclonal anti-GRP78 antibody (1:200; Santa Cruz Biotechnology) followed by biotinylated rabbit anti-goat IgG (1:800; DakoCytomation, Kyoto, Japan). Development was performed with peroxidase-conjugated avidin (Vector Laboratories, Burlingame, CA) and 3.3′-diaminobenzidine tetrahydrochloride (Wako, Osaka, Japan).

Statistical analysis. Values given in this study are presented as means ± SE of the results of independent three to four experiments. All analyses were performed by analysis of variance followed by Fisher's least significant different test. All statistical calculations were done with SPSS 16.0 for Windows.

RESULTS

ER stress suppressed basal and inducible EPO transcription in HepG2 cells. We assessed the change in EPO mRNA expression induced by ER stress in HepG2 exposed to the HIF stabilizer $CoCl_2$ or hypoxia (1% O_2). We used a noncytotoxic dose of an ER stressor, TUN or THG, as evaluated by LDH release assay in HepG2 cells exposed to $CoCl_2$ (7.4 ± 0.8 in nontreatment, 7.5 ± 0.6 in $CoCl_2$, 8.1 ± 0.9 in $CoCl_2$ + TUN, and 9.1 ± 0.5% in $CoCl_2$ + THG) or hypoxia (7.4 ± 0.8 in nontreatment, 8.2 ± 0.6 in hypoxia, 8.8 ± 0.3 in hypoxia + TUN, and 9.1 ± 0.4% in hypoxia + THG). The ER stress inducers activated the ER stress signal, namely the UPR, in cells under normoxia (not subjected to $CoCl_2$ or hypoxia), as shown by an increase in the expression of GRP78, which is an ER stress-inducible chaperone and used as an ER stress marker (Fig. 1*A*). Of note, ER stress markedly lowered the basal level of EPO transcription (Fig. 1*A*). As observed in normoxia, ER stress also dramatically lowered EPO mRNA expression induced by $CoCl_2$ or hypoxia (Fig. 1, *B* and *C*). This decrease in EPO transcription was negatively correlated with the level of UPR activation estimated by expression of GRP78 (Fig. 1, *B* and *C*). The change of EPO transcription was consistent with that of EPO protein production: the concentration of EPO protein in the culture supernatant of untreated HepG2 cells (culture for 24 h, 10.8 ± 1.0 mIU/ml) was significantly increased by exposure to 100 μM $CoCl_2$ for 24 h (47.0 ± 3.3 mIU/ml), while it was suppressed by treatment with 50 ng/ml THG (4.9 ± 1.0 mIU/ml; $P < 0.05$).

Importantly, the suppression of basal and inducible EPO transcription by ER stress was completely restored by the ER stress inhibitor salubrinal, which normalized the UPR state of ER stressor-treated HepG2 (Fig. 1*D*).

ER stress selectively suppressed EPO 3′-enhancer activity without affecting HIF directly. To identify the mechanisms of this decrease in EPO mRNA expression by ER stress in HepG2 cells, we assessed the transcriptional activity of a major EPO-enhancer region located in the 3′-downstream of the EPO gene (see Fig. 4*A*) by luciferase assay. EPO 3′-enhancer activity was enhanced by $CoCl_2$, while it was significantly dampened under ER stress conditions (Fig. 2*A*). ER stress per se also altered this enhancer activity under normoxia. This EPO 3′-enhancer activity is mainly regulated by HIF-2α through its binding to the HRE existing within this region (30, 40). We therefore evaluated the effect of ER stress on HIF-2α activity. Unexpectedly, ER stress did not interfere with the nuclear accumulation of HIF-2α induced by $CoCl_2$ (Fig. 2*B*); rather, it increased the nuclear accumulation of HIF-2α in both the presence and absence of $CoCl_2$. ER stress showed a similar effect in nuclear accumulation of HIF-1α (Fig. 2*C*), another isoform of HIF-α. Consistent with these observations, we also found that ER stress enhanced the level of HIF transactivation, as estimated by HRE-luciferase assay utilizing the reporter plasmid regulated by tandem copies of the HRE (37) (Fig. 2*D*). Of interest, while ER stress suppressed EPO expression, it markedly enhanced the expression of other HIF target genes, such as VEGF and GLUT1 (Fig. 2*E*). This was consistent with a previous finding that VEGF transcription was regulated by the UPR pathway as well as HIF pathway (11).

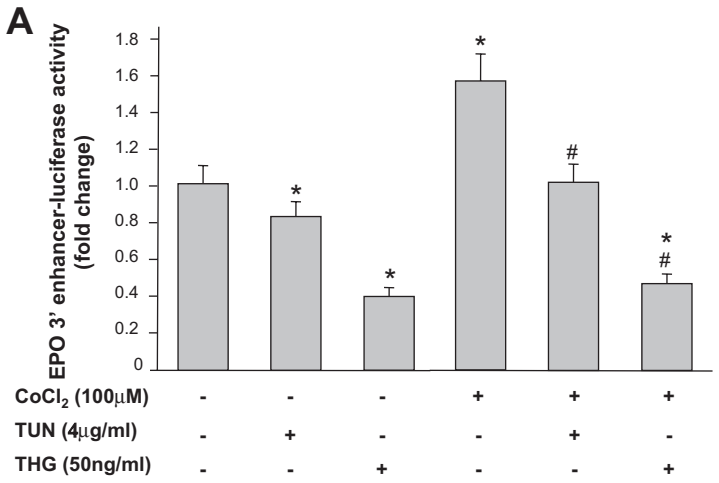

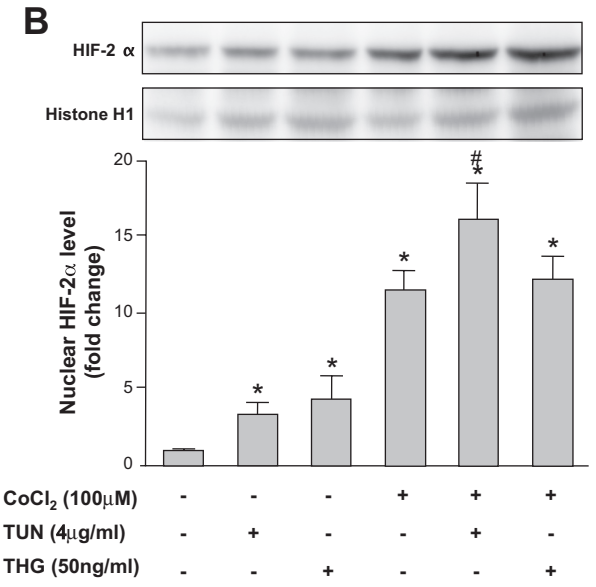

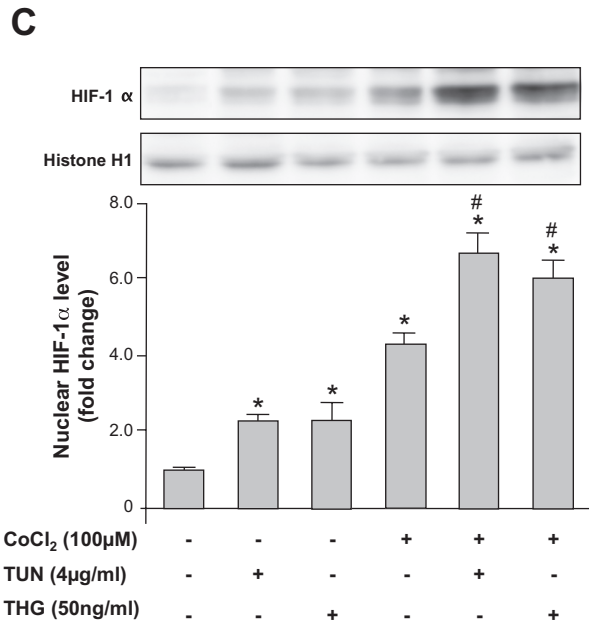

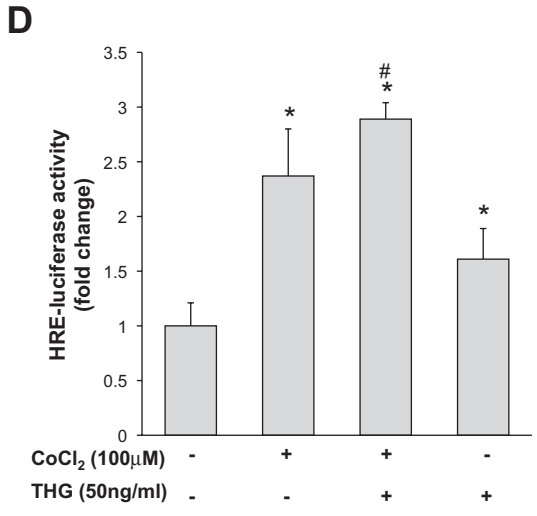

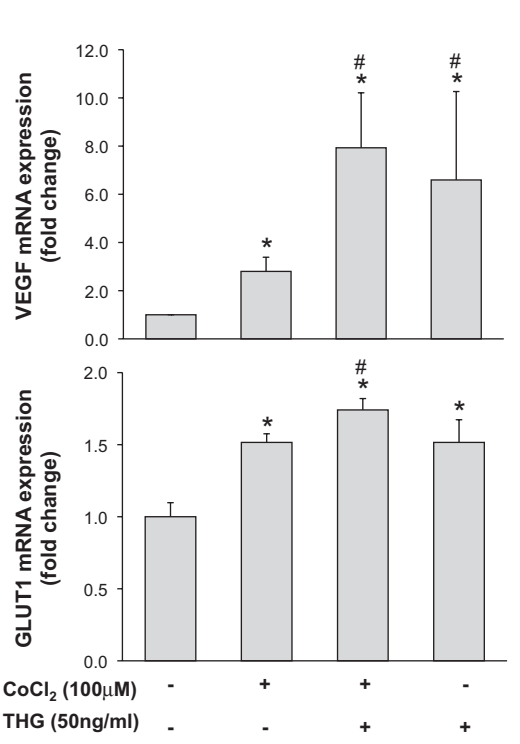

UPR transcription factor ATF4 suppressed EPO transcription via a decrease in EPO 3′-enhancer activity. From the findings that ER stress specifically decreased EPO transcription, but not other HIF target genes, we speculated that the UPR activation by ER stress impaired the oxygen-sensing machinery of EPO regulation by modulating EPO 3′-enhancer activity, without any direct effect on HIF. To evaluate the contribution of UPR to EPO 3′-enhancer activity, we conducted a transcription factor binding site search using a Transfac data base in this region. This revealed the existence of a putative binding element (TGACCTCT) of ATF4, a major transcription factor of the UPR pathway (25, 33), adjacent to HRE in the EPO 3′-enhancer region, indicating that ATF4 contributes to EPO transcription (see Fig. 4*A*). We therefore assessed the effect of ATF4 on EPO transcription in HepG2. ER stress inducers induced ATF4 activation, estimated by nuclear accumulation of ATF4, in parallel with suppression of EPO transcription (Fig. 3*A*). The ATF4 activation by ER stress was confirmed by an increase in phosphorylation of eIF2α, a major translation signal for ATF4, and CHOP mRNA expression, a representative ATF4-downstream target (Fig. 3*B*).

We further confirmed the effect of ATF4 on EPO transcription by gain-of-function analysis utilizing HepG2 overexpressing ATF4. ATF4 overexpression was evaluated by Western blot analysis for detection of nuclear ATF4 accumulation and subsequent ATF4-dependent luciferase activity utilizing a CHOP-luciferase reporter vector. Overexpression of ATF4 in HepG2 indeed increased nuclear accumulation of ATF4 (Fig. 3*C*) and thereby induced CHOP-luciferase activity under untreated and $CoCl_2$- or hypoxia-treated conditions compared with the wild-type cells (Fig. 3*D*). $CoCl_2$- or hypoxia-induced EPO mRNA expression was significantly decreased by ATF4 overexpression, as was observed under ER stress conditions (Fig. 3*E*). In parallel, ATF4 overexpression significantly decreased EPO 3′-enhancer activity but not HRE activity (Fig. 3*F*).

Because the putative binding element of ATF4 partly overlaps with DR-2 element, which augments hypoxic induction of EPO mRNA (18, 40) (Fig. 4*A*), it is difficult to confirm the suppressive effect of ATF4 on EPO production by utilizing the mutant of binding element. We thus employed the mutant of ATF4 (ATF4-mut) that lacks the transcriptional activity by deletion of the first 144 amino acids but retains the DNA binding element. While the ATF4-mut was markedly accumulated in the nuclei HepG2, the ATF4-mut did not enhance CHOP-luciferase activity, (Fig. 3, *C* and *D*). In contrast to ATF4, the ATF4-mut did not suppress basal and inducible EPO production (Fig. 3*E*). Further, the ATF4-mut affected neither EPO 3′-enhancer activity nor HRE activity (Fig. 3*F*). These results also supported the contribution of ATF4 on suppression of EPO production by UPR activation.

The expression level of ATF4 is mainly regulated by PERK-eIF2α pathway of UPR (25). We therefore performed loss-of-function analysis of ATF4 by utilizing HepG2 cells knocking down PERK by siRNA. When knockdown of PERK significantly decreased the activity of the PERK-eIF2α pathway, estimated by phosphorylation of eIF2α, and it thereby lowered the nuclear ATF4 accumulation (Fig. 3, *G*, *H*, and *I*). The decrease in ATF4 activity was confirmed by suppression of ATF4-downstream gene CHOP (Fig. 3*I*). Importantly, the suppression of ATF4 by ~65% inversely enhanced EPO transcription induced by $CoCl_2$ (Fig. 3*J*).

ATF4 bound to a novel ATF4 binding site in EPO 3′-enhancer region. Further, to confirm the interaction of ATF4 with the EPO 3′-enhancer region and to identify the ATF4 binding site within this region, we performed ChIP analysis using hypoxia-exposed HepG2 cells overexpressing FLAG-tagged ATF4. The results of ATF4 ChIP followed by PCR utilizing the primers Pr1 and Pr2 showed that ATF4 bound to the putative ATF binding element within the EPO 3′-enhancer region (Fig. 4, *A* and *B*). This finding was confirmed by real-time quantitative PCR utilizing other primer set (Pr3 and Pr4) and a TaqMan probe after ATF4 ChIP (Fig. 4, *A* and *C*).

Increased ER stress in rat liver and kidney impaired $CoCl_2$-induced EPO mRNA expression and plasma EPO levels. We next examined whether ER stress suppresses hepatic and renal EPO mRNA and plasma EPO levels in vivo. To induce ER stress in the liver and kidney, a nontoxic dose of TUN, which induces no functional or pathological changes in these organs, was injected intraperitoneally into the rats (15). Immunohistochemical analysis of GRP78 confirmed the induction of ER stress by TUN in hepatocytes of the liver or in interstitial cells of the kidney (Fig. 5*A*). $CoCl_2$ administration induced robust expression of hepatic EPO mRNA compared with untreated rats. As expected, further treatment of these $CoCl_2$-treated rats with TUN significantly blunted hepatic EPO transcription in association with an increase in the expression of GRP78 as well as CHOP (Fig. 5*B*). Similar results were observed in the kidney of the rats treated with $CoCl_2$ and TUN (Fig. 5*C*). In parallel, plasma EPO level was also increased by $CoCl_2$ and blunted by TUN (Fig. 5*D*). Overall, these in vivo data fully

Fig. 2. ER stress selectively suppressed EPO 3′-enhancer activity without affecting HIF directly. *A*: HepG2 cells transfected with the EPO 3′-enhancer reporter vector (pEPO3′-luc) were treated with $CoCl_2$ for 16 h in the presence or absence of TUN or THG, and then EPO 3′-enhancer-luciferase assay was performed. While $CoCl_2$ increased EPO-enhancer activity compared with untreated cells, it was significantly blunted by TUN or THG. The basal level of enhancer activity was also suppressed by ER stressors. *B*: to assess the nuclear translocation of HIF-2α in HegG2 treated with $CoCl_2$ under ER stress conditions, Western blot analysis utilizing the nuclear proteins followed by densitometry was performed. HIF stabilization by $CoCl_2$ for 12 h significantly enhanced the nuclear accumulation of HIF-2α compared with untreated cells. Of note, accumulation was further augmented by TUN or THG. TUN or THG per se also enhanced nuclear HIF-2α accumulation, with statistical significance. *C*: Western blot analysis for detection of the nuclear translocation of HIF-1α followed by densitometry revealed that $CoCl_2$ significantly upregulated the nuclear accumulation of HIF-1α in HepG2 cells compared with untreated cells. Of note, it was further augmented by TUN or THG. TUN or THG per se also induced HIF-1α accumulation with statistical significance. *D*: HepG2 cells transfected with hypoxia-responsive reporter (HRE) reporter vector (pHRE-luc) were treated with $CoCl_2$ for 16 h in the presence or absence of THG, and then HRE-luciferase assay was performed. $CoCl_2$-treated HepG2 cells showed the enhancement of HIF-α transactivation, as estimated by HRE-luciferase activity, compared with untreated cells. Transactivation was further enhanced by THG. THG per se also enhanced HRE-luciferase activity under normoxia. *E*: change in expression level of representative HIF-1α target genes VEGF (*top*) and GLUT1 (*bottom*) by ER stress was assessed by real-time PCR. $CoCl_2$ induced the expression of these target genes in HepG2 cells, and expression was further enhanced by THG. THG per se also induced VEGF and GLUT1 gene expressions. Each group consisted of 3 assays, and the experiments were independently repeated 4 times. *$P < 0.05$, compared with untreated cells; #$P < 0.05$, compared with cells exposed to $CoCl_2$ alone.

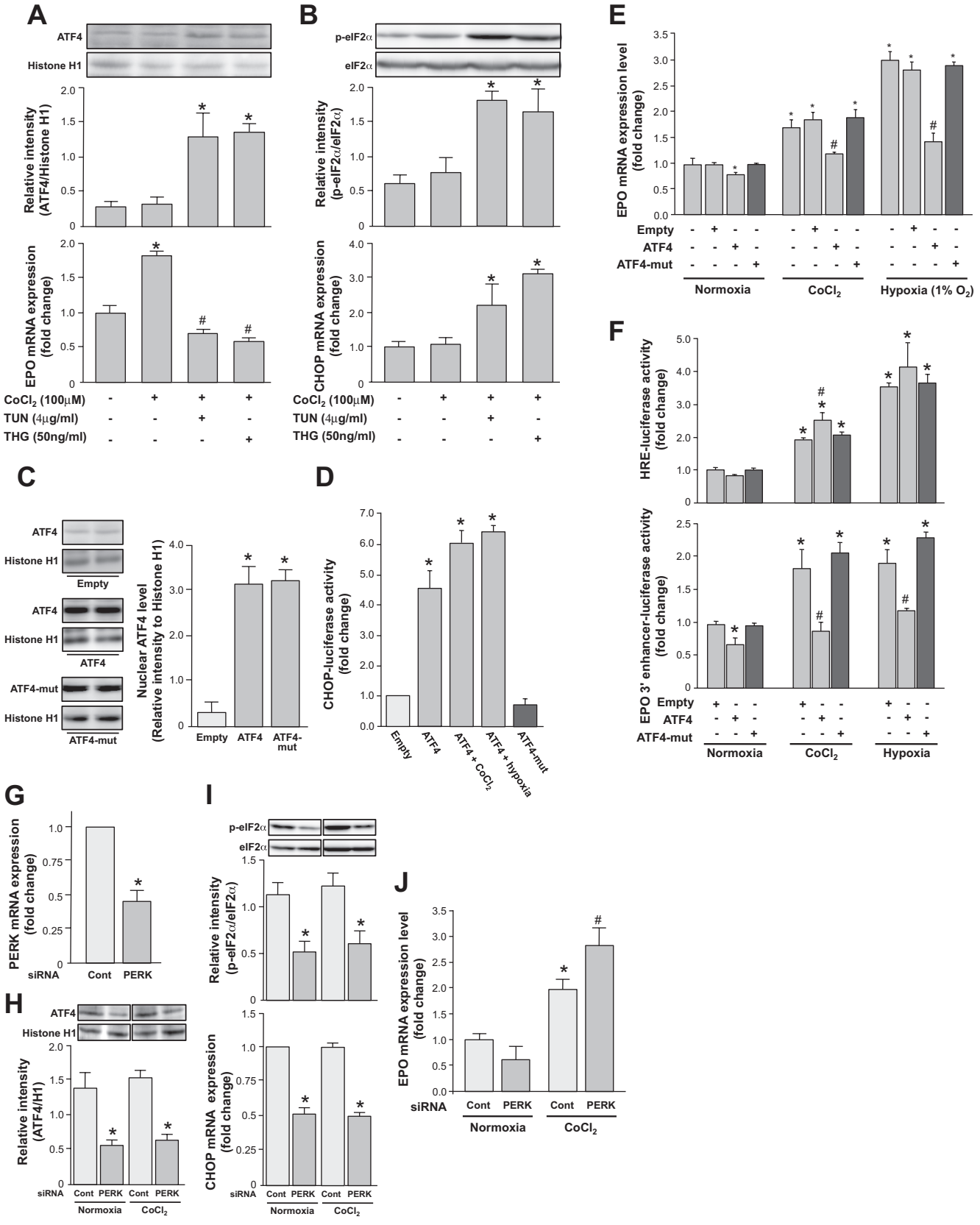

support the notion that the induction of ER stress and subsequent UPR activation impairs EPO production.

DISCUSSION

To date, a link between UPR activation induced by ER stress and EPO transcriptional regulation has not been reported. EPO production is predominantly regulated by HIF-2α, a master transcription factor for oxygen sensing machinery (24, 30, 40). We for the first time demonstrated that UPR activation acts to derange the transcriptional regulation of EPO and that overwhelming activation of the UPR transcription factor ATF4 contributes to the suppression of EPO mRNA expression under both normoxic and hypoxic conditions. Activation of ATF4 is regulated by PERK pathway and downregulation of PERK by siRNA indeed enhances EPO transcription in association with reduction of nuclear ATF4 level. Therefore, our current study strongly suggests that regulation of EPO transcription is orchestrated by both HIF-2α, a master transcription factor for oxygen-sensing machinery, and PERK-ATF4 axis of UPR pathway.

Transcriptional activity of HIF-2α is known to be modified under certain pathogenic conditions, including inflammation and oxidative stress associated with hyperglycemia (19, 23, 31, 38). Further, our recent study demonstrated the possibility of derangement of HIF-2α activity by uremic toxins (4). These pathogenic factors are also known as potent inducers of the ER stress signal (3, 7–9, 15–17, 20, 29). Although these findings suggest the link between HIF-2α activity and ER stress, the mechanism by which EPO production is impaired under ER stress conditions is not unclear. ER stress is significantly induced in various liver and kidney diseases and links to the progression of these diseases. Overwhelming activation of ATF4 in hepatic and renal EPO-producing cells may result in alteration of transcriptional regulation of EPO by oxygen-sensing machinery, HIF-2α pathway, and the subsequent insufficient EPO production leading to renal anemia.

Further, luciferase and ChIP assays revealed that UPR activation significantly suppresses EPO 3′-enhancer activity via the binding of ATF4 to a newly identified ATF4 binding element within the enhancer region. Our present study demonstrated that ER stress associated with UPR activation does not directly affect the nuclear accumulation of HIF-α in HepG2 cells under hypoxic conditions. This is consistent with our finding that UPR activation distinctly suppressed EPO transcription but not that of other HIF target genes, such as VEGF and GLUT1: rather, it enhanced mRNA expression of VEGF or GLUT1. EPO production under physiological hypoxic conditions might be negatively regulated by the UPR pathway as well as the HIF pathway. Therefore, it might be possible that various pathogens that trigger overwhelmed UPR activation derange EPO production.

Identification of a novel ATF4 binding site adjacent to HRE in the EPO 3′-enhancer region indicates the possibility that the interaction of ATF4 with this region may influence the 5′-promoter activity of EPO gene. HIF-α interacts with p300, a HIF coactivator, and the subsequent p300/HIF complex markedly enhances the 5′-promoter activity of EPO gene (39). Based on the fact that p300 also has an ATF4 binding site (12), the enhancer activity may be altered by the interaction of ATF4 with p300/HIF complex. This hypothesis is supported by the results of the experiments utilizing ATF4-mut: overexpression of ATF4-mut, which lacks the p300 binding site, did not suppress basal and inducible EPO transcription. Another possible mechanism of the effect of ATF4 on the EPO-enhancer activity is that the novel ATF4 binding site we found has an overlap with DR-2 element. DR-2 is an essential binding site of transcriptional factors that augment hypoxic induction of EPO mRNA (18, 40). For example, hepatocyte nuclear factor-4, a nuclear receptor protein, binds to DR-2 and dramatically increases the hypoxic inducibility of EPO production in hepatocytes (10, 40). Therefore, ATF4 may contribute to modulate the function of transcription factors bound to DR-2.

Fig. 3. Unfolded protein response (UPR) tactivating transcription factor (ATF)4 suppressed EPO transcription via a decrease in EPO 3′-enhancer activity without affecting HIF directly. *A*: level of nuclear accumulation of ATF4 was assessed by Western blot analysis. Nuclear accumulation of ATF4 was significantly increased in HepG2 treated with TUN or THG for 12 h, and it was associated with the suppression of EPO transcription induced by $CoCl_2$. *B*: activation of ATF4 by TUN or THG shown in Fig. 3*A* was confirmed by translation signal state of ATF4, estimated by phosphorylation of eukaryotic initiation factor-2α (eIF2α), and expression level of ATF4-downstream gene C/enhancer-binding protein homologous protein (CHOP). TUN or THG significantly induced phosphorylation of eIF2α (at 4 h of the exposure) and CHOP expression (at 12 h of the exposure), indicating the ATF4 activation by TUN or THG. *C* and *D*: HepG2 transfected with ATF4 or NH_2-terminal-deleted ATF4 (ATF4-mut) was verified by Western blot analysis for detection of nuclear accumulation of ATF4 (*C*) and its transcriptional activity as estimated by CHOP-lucilerase assay (*D*). Nuclear ATF4 accumulation in ATF4-transfected cells significantly increased transcriptional activity of ATF4 under normoxic or $CoCl_2$- or hypxioa-treated conditions. In contrast, ATF4-mut overexpression did not change the transcriptional activity, while it induced nuclear accumulation of ATF4-mut (ca. 32 kDa). Empty, empty vector alone; ATF4-mut, ATF4 lacking the first 144 amino acids and its transcriptional activity. *E*: HepG2 cells overexpressing ATF4 or ATF4-mut were treated with $CoCl_2$ or exposed to hypoxia for 12 h, and then EPO transcription level was assessed by real-time PCR. ATF4 overexpression significantly decreased the $CoCl_2$- or hypoxia-induced EPO mRNA expression. ATF4 also suppressed the basal level of EPO expression under normoxia. In contrast, ATF4-mut did not interfere both basal and inducible EPO transcriptional level. *F*: EPO 3′-enhancer-luciferase or HRE-luciferase assay was performed in HepG2 overexpressing ATF4 or ATF4-mut under various stimuli. ATF4 overexpression markedly suppressed EPO 3′-enhancer-luciferase activity but not HRE-luciferase activity, both of which were enhanced by $CoCl_2$ or hypoxia. Rather, ATF4 overexpression enhanced $CoCl_2$- or hypoxia-induced HRE-luciferase activity. ATF4 suppressed EPO 3′-enhancer activity under normoxia as well as under $CoCl_2$ treatment or hypoxia. In contrast, ATF4-mut overexpression did not change both EPO 3′-enhancer- and HRE-luciferase activities. *G-J*: HepG2 cells were transfected with small interfering (si)RNA for PERK, a translational regulator of ATF4, to downregulate the ATF4 activity and assessed basal and $CoCl_2$-induced EPO transcription level by real-time PCR. Expression of PERK was inhibited by siRNA specific for PERK but not by control siRNA (*G*). Level of suppression of ATF4 by PERK siRNA was evaluated at translation level of ATF4 (phosphorylation of eIF2α), the nuclear ATF4 accumulation, and transcriptional activity (CHOP expression; *H* and *I*) in HepG2 treated with TUN. TUN treatment was employed to emphasize the effect of PERK siRNA on suppression of ATF4. Nuclear ATF4 accumulation was decreased by PERK siRNA (*H*) and it was supported by both decreased phosphrylation of eIF2α (at 4 h of exposure to TUN), and decreased expression of ATF4-downstream target CHOP (at 12 h of exposure to TUN; *I*). Importantly, the suppression of ATF4 activity enhanced $CoCl_2$-induced EPO transcription in HepG2 in the absence of TUN (*J*). Each group consisted of 3 assays, and the experiments were independently repeated 4 times. Separated Western blot membranes are arranged as representative pictures of each group (*H* and *I*). $*P < 0.05$, compared with untreated cells; $\#P < 0.05$, compared with cells exposed to $CoCl_2$ or hypoxia alone.

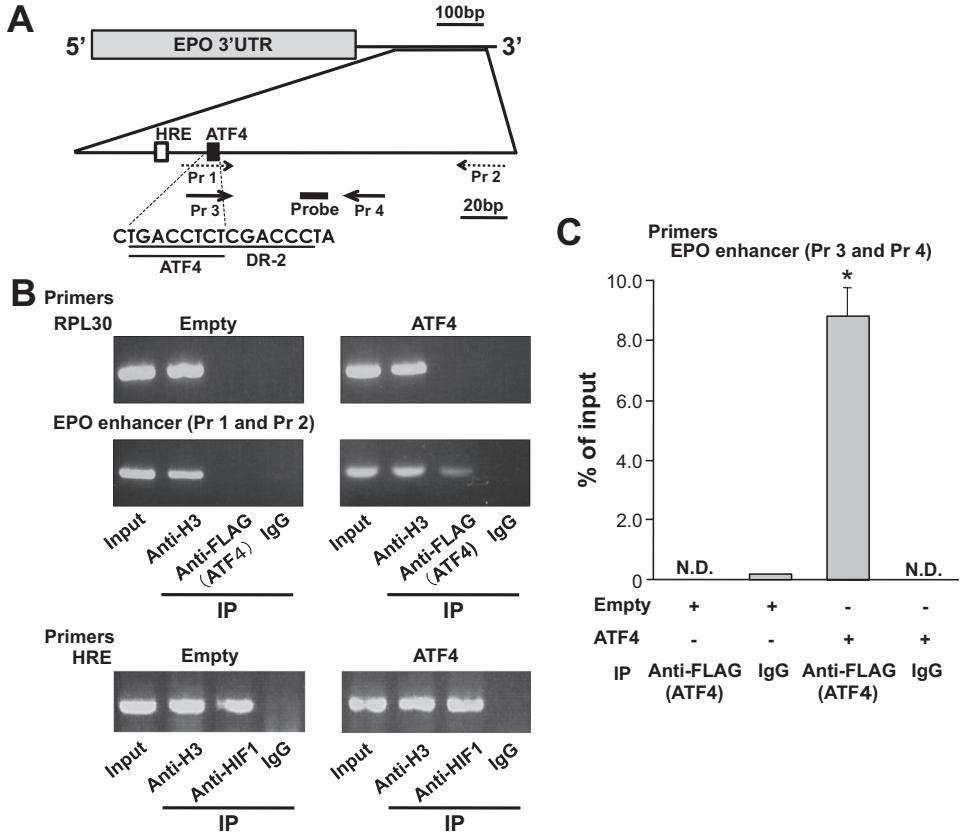

Fig. 4. Identification of a novel ATF4 binding site within the EPO 3′-enhancer region. *A*: schematic view of the EPO 3′-enhancer region. Locations of HRE and a putative ATF4 binding element in the EPO 3′-enhancer region are indicated by white and black boxes, respectively. Primers and a Taqman probe, which are used for chromatin immunoprecipitation (ChIP)-PCR and ChIP-real-time PCR, are indicated by arrows and a bold line, respectively. *B* and *C*: to reveal the binding of ATF4 to the putative binding site within the EPO 3′-enhancer region as shown in *A*, ChIP-PCR (*B*) or ChIP-real-time PCR (*C*) was performed utilizing ATF4 (FLAG-tagged)-overexpressing HepG2 cells. Digested chromatin from the cells (1×10^7), which were transfected with FLAG-tagged-ATF4 vector (ATF4) or mock (Empty) and subsequently exposed to hypoxia (1% O_2) for 8 h, was immunoprecipitated (IP) with anti-FLAG antibody, anti-histone H3 antibody (anti-H3, a positive control for IP), anti-HIF1 antibody (a positive control for IP of HRE located within 3′ EPO-enhancer region), or normal mouse IgG (IgG, a negative control for IP) and analyzed by PCR using 3′ EPO-enhancer region-specific primers (Pr 1 and Pr 2, *bottom left*) or the primers for the positive control (RPL30 or HRE). ATF4 ChIP using FLAG revealed enrichment of the putative ATF4 binding site adjacent to HRE in the EPO 3′-enhancer region (indicated by a black or white box in the schematic representation of EPO gene; *B*). ATF4 (FLAG) ChIP followed by quantitative real-time PCR using a TaqMan probe and independent primers (indicated by Probe, Pr 3, and Pr 4 in the schematic representation of EPO gene) also revealed the interaction of ATF4 transcription factor and putative ATF4 binding site in the EPO 3′-enhancer region (*C*). Experiments were independently repeated 3 times. $*P < 0.05$, compared with the control group utilizing the chromatin from mock-transfected cells and normal mouse IgG for IP.

In the previous study, it was demonstrated that ATF4 null fetuses were severely anemic because of an impairment in fetal-liver definitive hematopoiesis and the fetal livers of $ATF4^{-/-}$ mice were pale and hypoplastic (26). These data may support our findings that regulation of hepatic EPO production is impaired by ATF4 deficiency. Further investigation is necessary to improve our findings in in vivo study.

Kidney of patients with chronic kidney disease suffers from chronic hypoxia (13, 27, 28). Hypoxia signaling through the HIF and UPR pathways is carefully orchestrated for cell homeostasis (41). In particular, recent reports have demonstrated that ATF4 is degraded by prolyl hydroxylase (PHD), which regulates oxygen-dependent degradation of HIF (14, 21), suggesting that PHD regulates both HIF and UPR pathways in common. While inhibitor of PHD is highlighted as a stabilizer of HIF and a stimulator for EPO production (2), it may enhance the suppression of EPO transcription by ATF4. The function of PHD distinctly differs from the isoform of PHD (1). The expression level of each PHD isoform and the subsequent characteristics for regulation of HIF-1α or HIF-2α are variable in the different cells. Further analysis regarding PHD function to HIF-α and ATF4 in EPO-producing cells may help to understand the regulation of EPO production by HIF-2α and ATF4 under normal or pathogenic conditions.

Based on the previous reports that salubrinal increases ATF4 expression via the enhancement of phosphorylation of eIF2α (5), we also expected that salubrinal would further suppress EPO transcription in HepG2 treated with TUN. However, unexpectedly, we could not detect the further increase in nuclear ATF4 accumulation after 3–4 h of exposure to salubrinal (relative intensity of ATF4/histone H1 in TUN-treated HepG2 was 1.42 ± 0.17 and 1.40 ± 0.28 in the absence and presence of salubrinal, respectively). Meanwhile, salubrinal markedly suppressed TUN-induced ER stress after 24 h of the exposure in these cells (Fig. 1*D*). These data indicated that salubrinal did not dominantly activate eIF2α-ATF4 pathway, while it could suppress overwhelming UPR pathway of HepG2 induced by TUN. We speculate that an unknown inhibitory

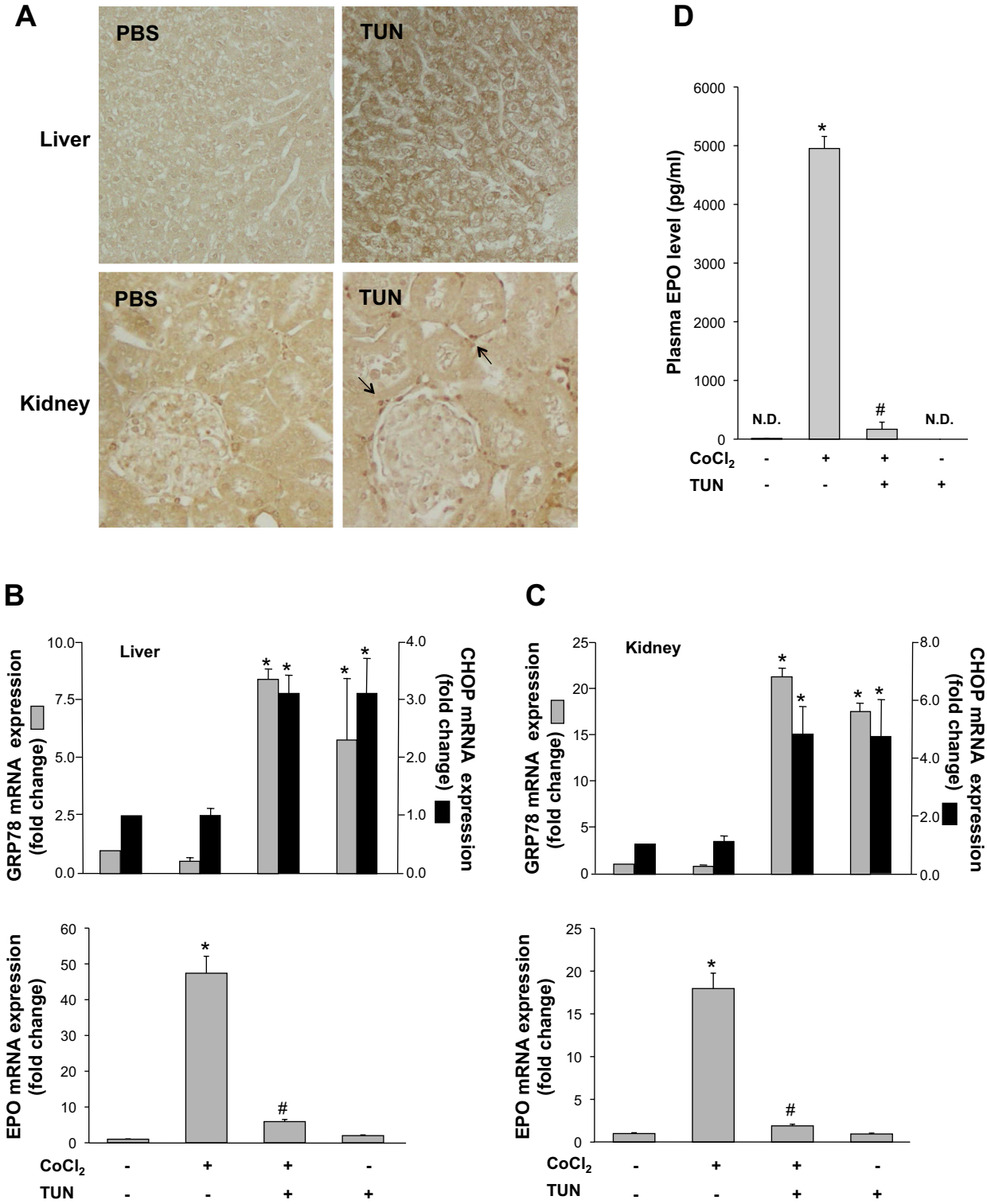

Fig. 5. Induction of ER stress in interstitial cells of rat kidney impaired $CoCl_2$-induced EPO mRNA expression and plasma EPO levels. *A*: rats were treated with $CoCl_2$ (60 mg/kg, subcutaneous injection) combined with intraperitoneal injection of PBS or TUN (0.3 mg/kg), and the liver and kidney was fixed with methyl Carnoy's solution. ER stress signal induction was assessed by immunohistochemical staining with anti-GRP78 antibody. A positive signal was predominantly observed in hepatocytes and the cells located in interstitium of the kidney (indicated by arrows). Original magnification, ×200. *B* and *C*: subcutaneous injection of $CoCl_2$ (60 mg/kg, 24 h) to rats induced elevations of hepatic (*B*) and renal (*C*) EPO mRNA levels, as measured by real-time PCR, compared with untreated control rats. Intraperitoneal injection of a nontoxic dose of TUN (0.3 mg/kg) to $CoCl_2$-treated rats significantly induced ER stress, as estimated by expression levels of GRP78 and CHOP, both in the liver and kidney. Importantly, this ER stress with UPR activation suppressed $CoCl_2$-induced hepatic and renal EPO transcription. *D*: ER stress induced by TUN markedly suppressed plasma EPO levels in $CoCl_2$-treated rats from 4,952.0 ± 173.0 to 169.0 ± 103.9 pg/ml. N.D.; not detectable. $*P < 0.05$, compared with the untreated control group; $\#P < 0.05$, compared with the group treated with $CoCl_2$ alone.

mechanism of salubrinal on UPR activation, one of which may have influence on negative feedback loop of the UPR pathway, might contribute to reverse the suppression of EPO production by ER stress. The diverse function of salubrinal is supported by the observation that the effect of salubrinal to ATF4 and GRP78 expression is discrepant in various cell types. In particular, the recent study showed that the increased level of ATF4 or GRP78 by $CdCl_2$ was not changed by salubrinal in human tubular cells (22). Another study demonstrated that salubrinal suppressed corticotropin releasing hormone-induced GRP78 expression in hippocampal neuronal cells (42).

In summary, ER stress selectively impairs EPO production but not that of other HIF target genes and modifies EPO 3′-enhancer activity by ATF4 binding to the enhancer region without interfering with HIF-2α directly. The UPR state, which maintains ER homeostasis, might play an important role in regulating the oxygen-sensing machinery for EPO transcription. This study highlights the possibility of novel strategies aimed at enhancing EPO production by targeting UPR molecules.

GRANTS

This work was supported by Grant-in-Aids for Scientific Research No. 22590880 (to R. Inagi) and 24390213 (to M. Nangaku) from the Japan Society for the Promotion of Science, Nakayama Foundation for Human Science (to R. Inagi), and Japanese Association of Dialysis Physicians (22051 to R. Inagi), and Kidney Foundation, Japan (JKFB12-5 to R. Inagi).

DISCLOSURES

No conflicts of interest, financial or otherwise, are declared by the author(s).

AUTHOR CONTRIBUTIONS

Author contributions: C.-K.C. and R.I. performed experiments; C.-K.C., M.N., T.T., and T.I. edited and revised manuscript; C.-K.C., M.N., T.T., T.I., and R.I. approved final version of manuscript; M.N., T.T., and T.I. interpreted results of experiments; R.I. conception and design of research; R.I. drafted manuscript.

REFERENCES

1. **Appelhoff RJ, Tian YM, Raval RR, Turley H, Harris AL, Pugh CW, Ratcliffe PJ, Gleadle JM.** Differential function of the prolyl hydroxylases PHD1, PHD2, and PHD3 in the regulation of hypoxia-inducible factor. *J Biol Chem* 279: 38458–3865, 2004.
2. **Bernhardt WM, Wiesener MS, Scigalla P, Chou J, Schmieder RE, Günzler V, Eckardt KU.** Inhibition of prolyl hydroxylases increases erythropoietin production in ESRD. *J Am Soc Nephrol* 21: 2151–2156, 2010.
3. **Chiang CK, Inagi R.** Glomerular diseases: genetic causes and future therapeutics. *Nat Rev Nephrol* 6: 539–554, 2010.
4. **Chiang CK, Tanaka T, Inagi R, Fujita T, Nangaku M.** Indoxyl sulfate, a representative uremic toxin, suppresses erythropoietin production in a HIF-dependent manner. *Lab Invest* 91: 1564–1571, 2011.
5. **Cnop M, Ladriere L, Hekerman P, Ortis F, Cardozo AK, Dogusan Z, Flamez D, Boyce M, Yuan J, Eizirik DL.** Selective inhibition of eukaryotic translation initiation factor 2 alpha dephosphorylation potentiates fatty acid-induced endoplasmic reticulum stress and causes pancreatic beta-cell dysfunction and apoptosis. *J Biol Chem* 282: 3989–3997, 2007.
6. **Correia SC, Moreira PI.** Hypoxia-inducible factor 1: a new hope to counteract neurodegeneration? *J Neurochem* 112: 1–12. 2010.
7. **Cunard R, Sharma K.** The endoplasmic reticulum stress response and diabetic kidney disease. *Am J Physiol Renal Physiol* 300: F1054–F1061, 2011.
8. **Cybulsky AV.** Endoplasmic reticulum stress in proteinuric kidney disease. *Kidney Int* 77: 187–193, 2010.
9. **Cybulsky AV, Takano T, Papillon J, Kitzler TM, Bijian K.** Endoplasmic reticulum stress in glomerular epithelial cell injury. *Am J Physiol Renal Physiol* 301: F496–F508, 2011.
10. **Galson DL, Tsuchiya T, Tendler DS, Huang LE, Ren Y, Ogura T, Bunn HF.** The orphan receptor hepatic nuclear factor 4 functions as a transcriptional activator for tissue-specific and hypoxia-specific erythropoietin gene expression and is antagonized by EAR3/COUP-TF1. *Mol Cell Biol* 15: 2135–2144, 1995.
11. **Ghosh R, Lipson KL, Sargent KE, Mercurio AM, Hunt JS, Ron D, Urano F.** Transcriptional regulation of VEGF-A by the unfolded protein response pathway. *PLos One* 5: e9575, 2010.
12. **Goodman RH, Smolik S.** CBP/p300 in cell growth, transformation, and development. *Genes Dev* 14: 1553–1577, 2000.
13. **Heyman SN, Khamaisi M, Rosen S, Rosenberger C.** Renal parenchymal hypoxia, hypoxia response and the progression of chronic kidney disease. *Am J Nephrol* 28: 998–1006, 2008.
14. **Hiwatashi Y, Kanno K, Takasaki C, Goryo K, Sato T, Torii S, Sogawa K, Yasumoto K.** PHD1 interacts with ATF4 and negatively regulates its transcriptional activity without prolyl hydroxylation. *Exp Cell Res* 317: 2789–2799, 2011.
15. **Inagi R, Kumagai T, Nishi H, Kawakami T, Miyata T, Fujita T, Nangaku M.** Preconditioning with endoplasmic reticulum stress ameliorates mesangioproliferative glomerulonephritis. *J Am Soc Nephrol* 19: 915–922, 2008.
16. **Inagi R.** Endoplasmic reticulum stress as a progression factor for kidney injury. *Curr Opin Pharmacol* 10: 156–165, 2010.
17. **Inagi R.** Inhibitors of advanced glycation and endoplasmic reticulum stress. *Methods Enzymol* 491: 361–80, 2011.
18. **Kambe T, Tada-Kambe J, Kuge Y, Yamaguchi-Iwai Y, Nagao M, Sasaki R.** Retinoic acid stimulates erythropoietin gene transcription in embryonal carcinoma cells through the direct repeat of a steroid/thyroid hormone receptor response element half-site in the hypoxia-response enhancer. *Blood* 96: 3265–3271, 2000.
19. **Katavetin P, Miyata T, Inagi R, Tanaka T, Sassa R, Ingelfinger JR, Fujita T, Nangaku M.** High glucose blunts vascular endothelial growth factor response to hypoxia via the oxidative stress-regulated hypoxia-inducible factor/hypoxia-responsible element pathway. *J Am Soc Nephrol* 17: 1405–1413, 2006.
20. **Kawakami T, Inagi R, Wada T, Tanaka T, Fujita T, Nangaku M.** Indoxyl sulfate inhibits proliferation of human proximal tubular cells via endoplasmic reticulum stress. *Am J Physiol Renal Physiol* 299: F568–F576, 2010.
21. **Köditz J, Nesper J, Wottawa M, Stiehl DP, Camenisch G, Franke C, Myllyharju J, Wenger RH, Katschinski DM.** Oxygen-dependent ATF-4 stability is mediated by the PHD3 oxygen sensor. *Blood* 110: 3610–3617, 2007.
22. **Komoike Y, Inamura H, Matsuoka M.** Effects of salubrinal on cadmium-induced apoptosis in HK-2 human renal proximal tubular cells. *Arch Toxicol* 86: 37–44, 2012.
23. **La Ferla K, Reimann C, Jelkmann W, Hellwig-Bürgel T.** Inhibition of erythropoietin gene expression signaling involves the transcription factors GATA-2 and NF-kappaB. *FASEB J* 16: 1811–1813, 2002.
24. **Lee FS, Percy MJ.** The HIF pathway and erythrocytosis. *Annu Rev Pathol* 6: 165–192, 2011.
25. **Malhi H, Kaufman RJ.** Endoplasmic reticulum stress in liver disease. *J Hepatol* 54: 795–809, 2011.
26. **Masuoka HC, Townes TM.** Targeted disruption of the activating transcription factor 4 gene results in severe fetal anemia in mice. *Blood* 99: 736–745, 2002.
27. **Mimura I, Nangaku M.** The suffocating kidney: tubulointerstitial hypoxia in end-stage renal disease. *Nat Rev Nephrol* 6: 667–678, 2010.
28. **Nangaku M.** Chronic hypoxia and tubulointerstitial injury: a final common pathway to end-stage renal failure. *J Am Soc Nephrol* 17: 17–25, 2006.
29. **Ohse T, Inagi R, Tanaka T, Ota T, Miyata T, Kojima I, Ingelfinger JR, Ogawa S, Fujita T, Nangaku M.** Albumin induces endoplasmic reticulum stress and apoptosis in renal proximal tubular cells. *Kidney Int* 70: 1447–1455, 2006.
30. **Paliege A, Rosenberger C, Bondke A, Sciesielski L, Shina A, Heyman SN, Flippin LA, Arend M, Klaus SJ, Bachmann S.** Hypoxia-inducible factor-2alpha-expressing interstitial fibroblasts are the only renal cells that express erythropoietin under hypoxia-inducible factor stabilization. *Kidney Int* 77: 312–318, 2010.
31. **Rosenberger C, Khamaisi M, Abassi Z, Shilo V, Weksler-Zangen S, Goldfarb M, Shina A, Zibertrest F, Eckardt KU, Rosen S, Heyman SN.** Adaptation to hypoxia in the diabetic rat kidney. *Kidney Int* 73: 34–42, 2008.
32. **Rosmorduc O, Housset C.** Hypoxia: a link between fibrogenesis, angiogenesis, and carcinogenesis in liver disease. *Semin Liver Dis* 30: 258–270, 2010.
33. **Rouschop KM, van den Beucken T, Dubois L, Niessen H, Bussink J, Savelkouls K, Keulers T, Mujcic H, Landuyt W, Voncken JW, Lambin P, van der Kogel AJ, Koritzinsky M, Wouters BG.** The

unfolded protein response protects human tumor cells during hypoxia through regulation of the autophagy genes MAP1LC3B and ATG5. *J Clin Invest* 12: 127–141, 2010.
34. **Samuel VT, Shulman GI.** Mechanisms for insulin resistance: common threads and missing links. *Cell* 148: 852–871, 2012.
35. **Semenza GL.** Hypoxia-inducible factor 1: regulator of mitochondrial metabolism and mediator of ischemic preconditioning. *Biochim Biophys Acta* 1813: 1263–1268, 2011.
36. **Tabas I, Ron D.** Integrating the mechanisms of apoptosis induced by endoplasmic reticulum stress. *Nat Cell Biol* 13: 184–190, 2011.
37. **Tanaka T, Miyata T, Inagi R, Fujita T, Nangaku M.** Hypoxia in renal disease with proteinuria and/or glomerular hypertension. *Am J Pathol* 165: 1979–1992, 2004.
38. **Thangarajah H, Yao D, Chang EI, Shi Y, Jazayeri L, Vial IN, Galiano RD, Du XL, Grogan R, Galvez MG, Januszyk M, Brownlee M, Gurtner GC.** The molecular basis for impaired hypoxia-induced VEGF expression in diabetic tissues. *Proc Natl Acad Sci USA* 106: 13505–13510, 2009.
39. **Wang F, Zhang R, Wu X, Hankinson O.** Roles of coactivators in hypoxic induction of the erythropoietin gene. *PLos One* 5: e10002, 2010.
40. **Weidemann A, Johnson RS.** Nonrenal regulation of EPO synthesis. *Kidney Int* 75: 682–688, 2009.
41. **Wouters BG, Koritzinsky M.** Hypoxia signalling through mTOR and the unfolded protein response in cancer. *Nat Rev Cancer* 8: 851–864, 2008.
42. **Zhang Y, Liu W, Ma C, Geng J, Li Y, Li S, Yu F, Zhang X, Cong B.** Endoplasmic reticulum stress contributes to CRH-induced hippocampal neuron apoptosis. *Exp Cell Res* 318: 732–740, 2012.